# Does Retinal Vascular Geometry Vary with Cardiac Cycle?

*Hao Hao,*[1,9] *Muhammad B. Sasongko,*[2,3,9] *Tien Y. Wong,*[2,4,5] *Mohd Zulfaezal Che Azemin,*[1,6] *Behzad Aliahmad,*[1] *Lauren Hodgson,*[2] *Ryo Kawasaki,*[2] *Carol Y. Cheung,*[4,5] *Jie Jin Wang,*[2,8] *and Dinesh K. Kumar*[1]

**Purpose.** Changes in retinal vascular parameters have been shown to be associated with systemic vascular diseases. In this study, we assessed the physiologic variations in retinal vascular measurements during the cardiac cycle.

**Methods.** Fundus images were taken using electrocardiogram-synchronized retinal camera at nine distinct cardiac points from 15 healthy volunteers (135 images). Analyses of retinal vessel geometric measures, including retinal vessel caliber (individual and summary), tortuosity, branching angle, length–diameter ratio (LDR), and optimality deviation, were performed using semiautomated computer software. Repeated-measures ANOVAs were used to obtain the means and to estimate the variation of each cardiac point compared with cardiac point 1.

**Results.** There was a significant variation of the caliber of the individual arteriolar and venular vessels. However, there was no significant variation found for vessel caliber summary, represented by the central retinal arteriolar equivalent (CRAE) and the central retinal venular equivalent (CRVE). There was also no significant variation found for tortuosity and branching angle, and LDR showed none or very little variations at different cardiac points: variations in caliber ranges between 0 and 4.1%, tortuosity 0 and 1.5%, branching angle 0 and 3.5%, and LDR 0 and 2%; all values for variations, $P > 0.1$; linear trend, $P > 0.5$; and nonlinear trend, $P > 0.8$.

**Conclusions.** This study showed that there were minimal variations in the CRAE, CRVE, tortuosity, and branching angle that are clinically used for two-dimensional measures of retinal vascular geometry during cardiac cycles. However, there was significant variation in the caliber of the individual vessels over the cardiac cycle. (*Invest Ophthalmol Vis Sci.* 2012;53:5799–5805) DOI:10.1167/iovs.11-9326

Since the past decade, advances in retinal imaging technique have allowed direct, in vivo observations of the human circulation system. A number of studies have demonstrated that quantitative measurement of retinal vascular geometric parameters from fundus photographs, including caliber, tortuosity, and length–diameter ratio (LDR), are strongly associated with blood pressure,[1–3] major systemic vascular diseases including coronary heart disease,[4] ischemia heart diseases,[5] and diabetes mellitus[6] and its complications.[7,8] Consistent with these, it has been suggested that such geometric parameters reflect the optimality state of the peripheral (retina) circulation[9] and, therefore, hemodynamic changes associated with pathophysiologic processes (i.e., blood pressure, diabetes, inflammation, and other mechanisms) may alter the geometric organization (e.g., dilated vessels, more tortuous, wider branching angle, low LDR, fractal dimension) of the retinal vasculature.[1,3,5,7,10]

Physiologically, a spontaneous increase in blood volumetric flow entering the ophthalmic vascular system is expected during the peak-systolic phase of the cardiac cycle, and lower flow may occur during the diastolic phase.[11] Furthermore, blood flow changes would correspond to variations in intravascular pressure, which may induce vasomotor responses to adjust its diameter size.[11] Although previous studies have shown that static measures of retinal vessel caliber varied at different points over the cardiac cycle,[12–14] variations in other retinal vascular geometric parameters (tortuosity, branching angle, LDR, and optimality deviation) during the cardiac cycle have never been investigated.

Considering the potential variations of retinal vascular geometry resulting from the ambient hemodynamic during the cardiac cycle, understanding temporal changes during normal cardiac rhythm is important to ensure that observed changes in retinal vascular geometry in relation to several diseases are due to specific pathologic conditions, but not physiologic variations. It is important to determine the inherent variations in the current static retinal imaging technique, where the image is obtained without considering the temporal location of the sample with respect to the cardiac cycle. In this study, we have investigated the variation of retinal vascular geometric parameters (vessel caliber, tortuosity, branching angle, LDR, and optimality deviation), quantitatively measured from electrocardiogram (ECG)-synchronized fundus photographs, during a normal cardiac cycle in generally healthy participants.

From the [1]School of Electrical and Computer Engineering, Royal Melbourne Institute of Technology (RMIT University), Melbourne, Australia; the [2]Centre for Eye Research Australia, Royal Victorian Eye and Ear Hospital, University of Melbourne, Melbourne, Australia; the [3]Department of Ophthalmology, Faculty of Medicine, Gadjah Mada University, Yogyakarta, Indonesia; the [4]Singapore Eye Research Institute, Singapore National Eye Centre, Singapore; the [5]Department of Ophthalmology, Yong Loo Lin School of Medicine, National University of Singapore, Singapore; the [6]Department of Allied Health Sciences, International Islamic University Malaysia, Pahang, Malaysia; the [7]School of Computing, National University of Singapore, Singapore; and the [8]Centre for Vision Research, Westmead Millennium Institute, University of Sydney, Sydney, Australia.

[9]These authors contributed equally to the work presented here and should therefore be regarded as equivalent authors.

Supported in part by the Victorian Government and the National Health and Medical Research Council Centre for Clinical Research Excellence/Translational Clinical Research in Major Eye Diseases Grant 529923.

Submitted for publication December 14, 2011; revised April 1, 2012; accepted July 13, 2012.

Disclosure: **H. Hao**, None; **M.B. Sasongko**, None; **T.Y. Wong**, None; **M.Z. Che Azemin**, None; **B. Aliahmad**, None; **L. Hodgson**, None; **R. Kawasaki**, None; **C.Y. Cheung**, None; **J.J. Wang**, None; **D.K. Kumar**, None

Corresponding author: Dinesh K. Kumar, RMIT University, 124 Latrobe Street, Melbourne, Victoria, Australia 3000; dinesh@rmit.edu.au.

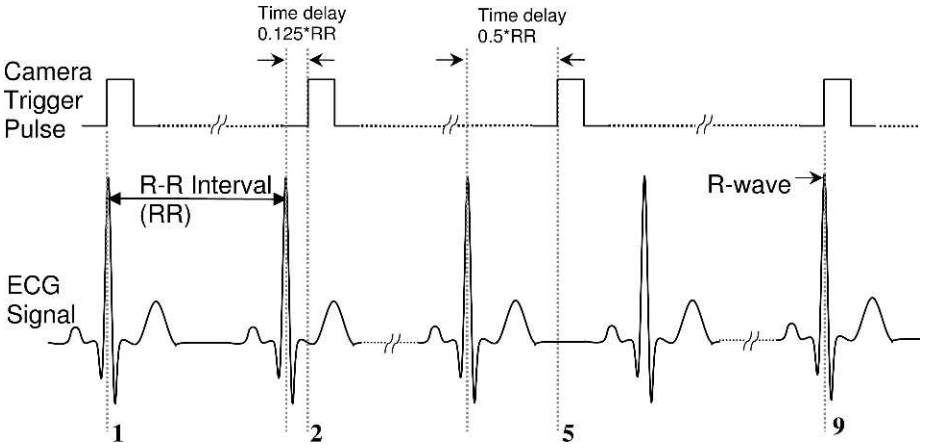


**Figure 1.** Time delay calculation and cardiac cycle points when fundus images were captured. The first and ninth points correspond to the R-wave and the other seven points are equally distributed over the cardiac cycle. For the camera triggering point $n$, the image is photographed at a time delay of $(n-1)\times 0.125\times \mathrm{RR}$ after the R-wave. This figure illustrates the outputs of the ECG signal and the trigger pulse at the first, second, fifth, and ninth points.

## Materials and Methods

### Study Participants

This study was approved by the RMIT University Research Ethics Committee and conducted in accordance with the principles of the Declaration of Helsinki of 1975, as revised in 2008. A written consent form was obtained from each participant. Fifteen volunteers (25–45 years of age; mean 33 years; 11 males and 4 females) were recruited to participate in this study. The exclusion criteria were subjects having the following conditions: prescribed or other medication on the day of the experiment, hypertension, history of cardiovascular disease, diabetes, current smoker, eye disease, and eye surgery. Nine disc-centered fundus images of the nondilated left eye of each participant (a total of 135 disc-centered fundus images) were captured using the ECG-synchronized retinal photography module (described in the following text) at nine distinct points during the cardiac cycle, the first and ninth corresponding to the R-wave, and the other seven equally distributed over the cardiac cycle (Fig. 1).

### ECG-Synchronized Retinal Photography

A three-lead ECG monitoring device, along with a purpose-built microcontroller (Arduino Uno, www.arduino.cc), was used to identify the R-wave and obtain the R–R interval in real time, and to generate a trigger pulse for acquiring the retinal image (Fig. 2). A digital 45° nonmydriatic retinal camera (Canon CR-1; Canon Inc., Tokyo, Japan) was used to capture the retinal image. The triggering mechanism was electronically connected with the ECG synchronization unit and this allowed for automatic triggering of the camera. The ECG signal and triggering pulse were monitored on an oscilloscope by the examiner during the experiment, and recorded along the retinal images on the laptop computer with a timestamp. This ensured that the retinal imaging was synchronized with the cardiac cycle.

Based on the typical resting heart rate of 60 to 100 beats/min in adults, the R–R interval was considered to be abnormal if the detected R–R interval was greater than 1000 or less than 600 milliseconds. No retinal image was taken in such a case and an alarm was raised for the examiner.

### Measurement of Individual Vessel Diameter

The diameter of the individual vessel at a single cross-section was measured using specially developed software. This software measured a vessel segment approximately 1 to 2 disk diameters from the optic nerve head (Fig. 3a). The location on the vessel was manually located

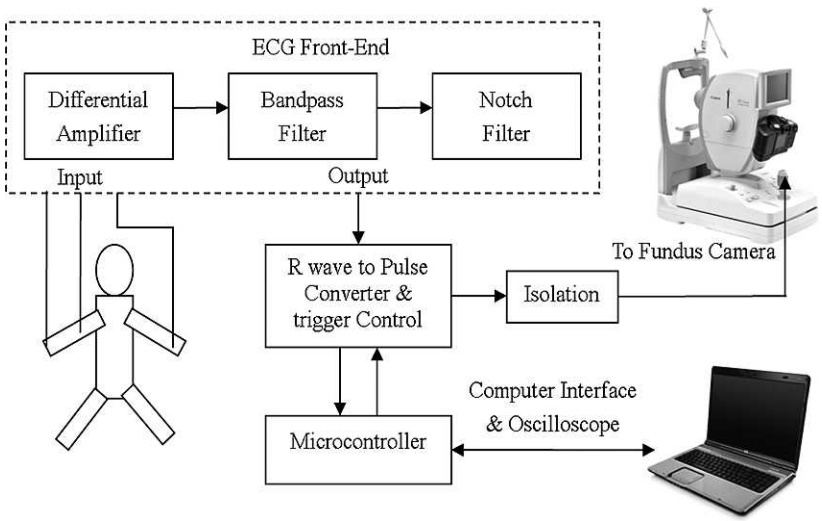


**Figure 2.** ECG synchronized retinal photography system.

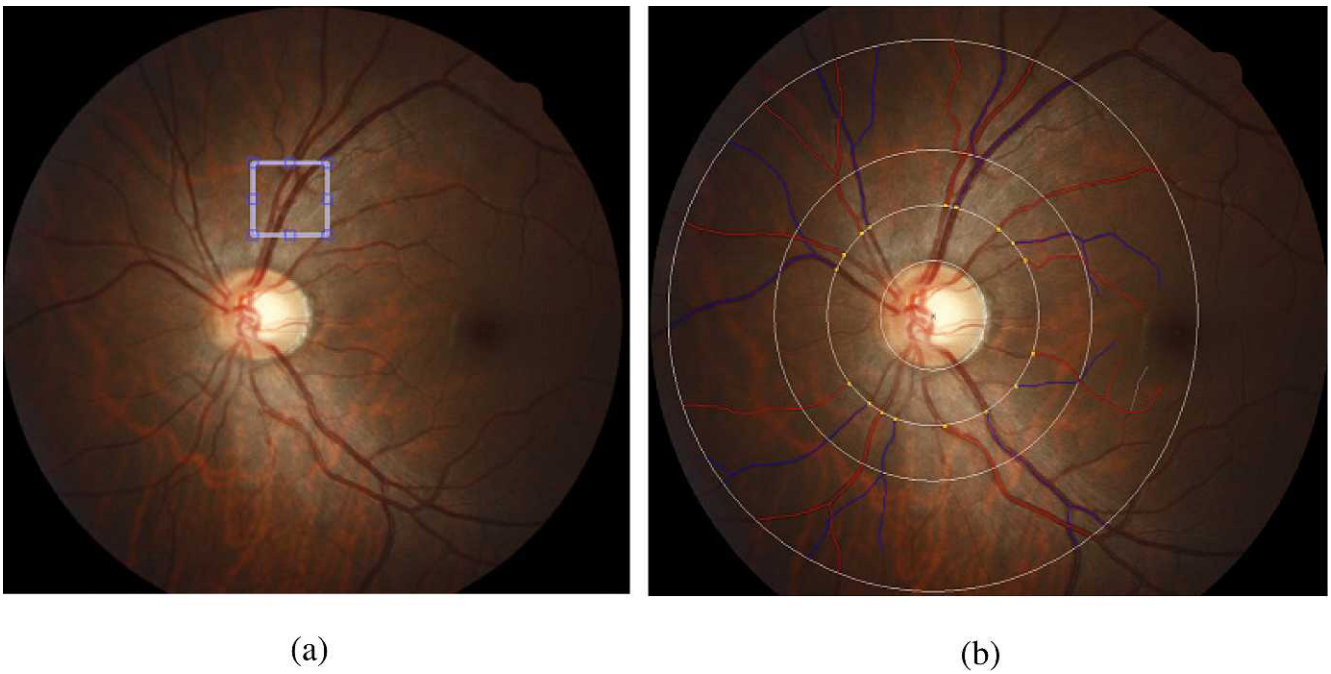


**Figure 3.** Vessel diameter measurement sites. (**a**) Individual vessel diameter measurements were calculated from 20 cross-sections from arteriole and venule segments. (**b**) Vessel diameter summary calculated based on CRAE and CRVE formulas.

in the first frame such that the region was noise free, and 20 cross-sectional profiles of the vessel were obtained and modeled using a combination of Gaussian and twin-Gaussian functions.[15] The diameter of the vessel was estimated as the maximum distance between a pair of two peaks of the second-order derivatives of the Gaussian model. The other eight frames were registered automatically to the first frame using an image registration and montage algorithm software package (DualAlign i2k Retina; Topcon Medical Systems, Oakland, NJ) based on an algorithm detailed in the previous work,[16] to ensure the sampling of the cross-sections at the same spatial location.

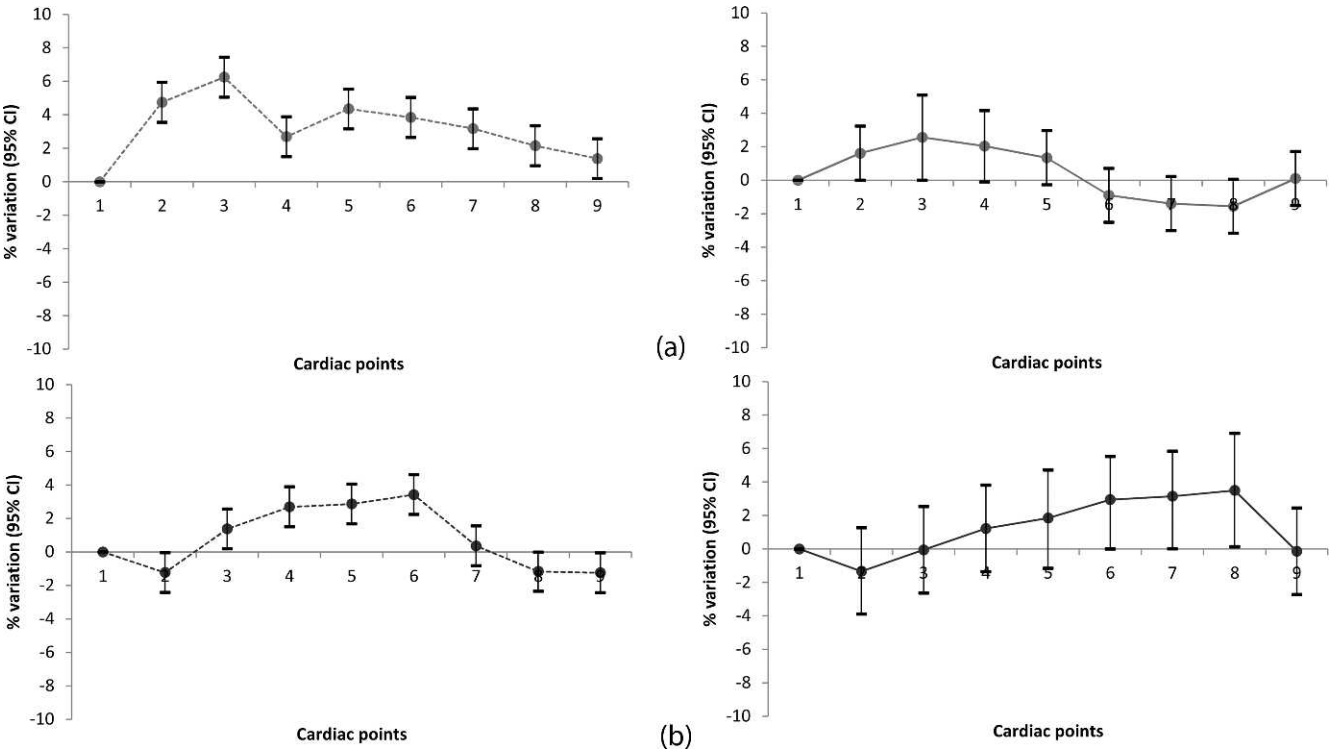


**Figure 4.** Variations of summary of individual vessel caliber and vessel caliber summary (CRAE and CRVE) at different cardiac points. (**a**) Arteriole caliber change across cardiac cycle, and (**b**) venule caliber change across cardiac cycle.

**Table.** Variation of Retinal Vascular Parameters in Different Cardiac Cycle Points Compared with Baseline (Cycle Reference Point 1)

| | | Arterioles | | Venules | |
|---|---|---|---|---|---|
| **Vascular Parameters (unit)** | **Cycle Point** | **Mean (SD)** | **% Variation*** | **Mean (SD)** | **% Variation*** |
| Individual vessel caliber (microns) | | *P* value† < 0.001 | | *P* value† < 0.001 | |
| | 1 | 67.6 (8.00) | reference | 88.0 (14.7) | reference |
| | 2 | 70.7 (11.0) | 4.7 | 86.8 (14.5) | 1.2 |
| | 3 | 71.5 (12.8) | 6.3 | 89.1 (15.6) | 1.4 |
| | 4 | 69.3 (9.30) | 2.7 | 90.3 (15.7) | 2.7 |
| | 5 | 70.6 (11.3) | 4.4 | 90.7 (17.4) | 2.9 |
| | 6 | 70.1 (9.70) | 3.8 | 91.0 (16.0) | 3.4 |
| | 7 | 69.6 (9.80) | 3.2 | 88.1 (14.4) | 0.4 |
| | 8 | 69.0 (9.50) | 2.2 | 86.9 (15.0) | 1.2 |
| | 9 | 68.7 (10.3) | 1.4 | 86.9 (16.1) | 1.2 |
| Summary of vessel caliber | | *P* value† = 0.52 | | *P* value† = 0.12 | |
| | 1 | 151.1 (13.3) | reference | 216.4 (17.5) | reference |
| | 2 | 153.5 (13.3) | 1.6 | 214.6 (15.9) | 0.8 |
| | 3 | 154.9 (13.6) | 2.5 | 217.4 (16.9) | 0.5 |
| | 4 | 154.1 (13.4) | 2.0 | 220.2 (17.3) | 1.8 |
| | 5 | 153.1 (14.8) | 1.3 | 221.6 (17.3) | 2.4 |
| | 6 | 149.7 (14.0) | 0.9 | 223.9 (17.1) | 3.5 |
| | 7 | 148.9 (13.9) | 1.4 | 224.5 (18.2) | 3.8 |
| | 8 | 148.8 (15.5) | 1.5 | 225.1 (18.0) | 4.1 |
| | 9 | 151.2 (13.0) | 0.0 | 217.3 (17.9) | 0.4 |
| S. tortuosity (index) | | *P* value† = 0.93 | | *P* value† = 0.92 | |
| | 1 | 1.09 (0.02) | reference | 1.10 (0.01) | reference |
| | 2 | 1.09 (0.02) | 0.0 | 1.10 (0.02) | 0.2 |
| | 3 | 1.09 (0.02) | 0.0 | 1.10 (0.02) | 0.0 |
| | 4 | 1.09 (0.02) | 0.0 | 1.10 (0.01) | 0.1 |
| | 5 | 1.09 (0.02) | 0.0 | 1.10 (0.01) | 0.0 |
| | 6 | 1.09 (0.02) | 0.0 | 1.10 (0.02) | 0.0 |
| | 7 | 1.09 (0.02) | 0.0 | 1.10 (0.02) | 0.0 |
| | 8 | 1.09 (0.02) | 0.0 | 1.10 (0.02) | 0.0 |
| | 9 | 1.09 (0.02) | 0.0 | 1.10 (0.02) | 0.1 |
| C. tortuosity ($\times 10^5$) | | *P* value† = 0.97 | | *P* value† = 0.91 | |
| | 1 | 5.93 (1.15) | reference | 6.52 (0.60) | reference |
| | 2 | 5.93 (1.20) | 0.0 | 6.59 (0.79) | 1.1 |
| | 3 | 5.86 (1.17) | 0.9 | 6.47 (0.64) | 0.7 |
| | 4 | 5.89 (1.08) | 0.3 | 6.57 (0.69) | 0.6 |
| | 5 | 5.92 (1.22) | 0.2 | 6.50 (0.68) | 0.1 |
| | 6 | 5.88 (1.11) | 0.4 | 6.32 (0.72) | 1.1 |
| | 7 | 6.00 (1.16) | 1.5 | 6.59 (0.70) | 1.3 |
| | 8 | 5.83 (1.04) | 1.1 | 6.52 (0.64) | 0.0 |
| | 9 | 5.88 (1.07) | 0.3 | 6.52 (0.64) | 0.0 |
| Branching angle (degree) | | *P* value† = 0.88 | | *P* value† = 0.19 | |
| | 1 | 76.9 (22.7) | reference | 82.2 (7.25) | reference |
| | 2 | 76.0 (21.9) | 0.7 | 80.3 (13.3) | 2.3 |
| | 3 | 75.5 (21.9) | 1.3 | 80.9 (13.4) | 1.5 |
| | 4 | 76.7 (23.1) | 0.0 | 81.2 (11.2) | 1.2 |
| | 5 | 76.4 (23.1) | 0.0 | 79.2 (11.6) | 3.4 |
| | 6 | 75.4 (21.5) | 0.2 | 84.5 (8.81) | 2.9 |
| | 7 | 77.3 (23.5) | 0.8 | 82.4 (13.2) | 0.8 |
| | 8 | 77.5 (22.6) | 1.2 | 81.4 (7.44) | 1.0 |
| | 9 | 75.3 (25.5) | 0.4 | 82.4 (13.1) | 0.1 |
| LDR | | *P* value† = 0.84 | | *P* value† = 0.90 | |
| | 1 | 2.52 (0.89) | reference | 2.88 (0.11) | reference |
| | 2 | 2.47 (0.89) | 1.9 | 2.90 (0.25) | 0.6 |
| | 3 | 2.56 (0.85) | 1.5 | 2.84 (0.11) | 1.3 |
| | 4 | 2.52 (0.67) | 0.0 | 2.89 (0.10) | 0.3 |
| | 5 | 2.57 (0.84) | 1.9 | 2.91 (0.11) | 1.0 |
| | 6 | 2.56 (0.84) | 1.5 | 2.89 (0.09) | 0.3 |
| | 7 | 2.56 (0.90) | 1.5 | 2.87 (0.11) | 0.3 |
| | 8 | 2.52 (0.81) | 0.0 | 2.89 (0.11) | 0.3 |
| | 9 | 2.52 (0.89) | 0.0 | 2.89 (0.12) | 0.3 |

**Table.** Continued

| Vascular Parameters (unit) | Cycle Point | Arterioles | | Venules | |
|---|---|---|---|---|---|
| | | Mean (SD) | % Variation* | Mean (SD) | % Variation* |
| Optimality deviation | | *P* value† = 0.84 | | *P* value† = 0.15 | |
| | 1 | −0.47 (0.34) | reference | −0.41 (0.35) | reference |
| | 2 | −0.45 (0.30) | 4.2 | −0.38 (0.30) | 7.3 |
| | 3 | −0.50 (0.35) | 6.4 | −0.38 (0.30) | 7.3 |
| | 4 | −0.46 (0.37) | 2.1 | −0.38 (0.39) | 7.3 |
| | 5 | −0.32 (0.38) | 32.0 | −0.33 (0.29) | 19.5 |
| | 6 | −0.36 (0.32) | 23.4 | −0.29 (0.31) | 29.2 |
| | 7 | −0.38 (0.36) | 19.1 | −0.26 (0.37) | 36.6 |
| | 8 | −0.40 (0.41) | 14.9 | −0.33 (0.32) | 19.5 |
| | 9 | −0.47 (0.36) | 0.0 | −0.41 (0.32) | 0.0 |

Mean, SD, and all *P* values were estimated using repeated measures ANOVA. S. tortuosity, simple tortuosity; C. tortuosity, curvature tortuosity; LDR, length to diameter ratio.

* Absolute value compared to cycle point 1.

† Overall *P* value for variations.

## Measurement of Retinal Vascular Geometry Using SIVA

Measurement of other retinal vascular geometric properties was performed quantitatively using a semiautomated computerized system (Singapore "I" Vessel Assessment [SIVA] version 3.0, Singapore) following a standardized protocol.[3,7,8] The grading was performed on one image at a time and, during the grading, the other images were masked to avoid any bias. Furthermore, to eliminate potential systematic error, the order of the image frames (1 to 9) for grading was not sequential but randomized. Images were considered as "poor quality" if they were blurred or an incomplete representation of zone C, and as "ungradable" if there were fewer than four large gradable arterioles or venules.

Measurements were based on a summary of the arterioles and venules separately. The software combined the individual measurement into summary indices for caliber, tortuosity, branching angles, LDR, and optimality deviation separately. The technical details of these parameters are as provided in the following text, and described in previous publications.[17–20]

## Brief Description of SIVA

The SIVA measurement technique has been described previously.[3,7,8] Briefly, the SIVA measures retinal microvascular geometric parameters within a concentric zone between the optic disc margin and 2 optic disc diameters away from the optic disc margin. The software automatically detects the center of the optic disc and divides the region into three concentric subzones (A, B, C) surrounding the optic disc, each zone corresponding to the area between optic disc margin to 0.5 optic disc diameter, 0.5 to 1.0 disc diameter, and 0.5 to 2.0 optic disc diameters away from the optic disc margin. The grader confirms the correct detection of the optic disc and the three concentric subzones by the program, and then the grader executes the program to generate a line tracing of the retinal vessels. This software also has an automated function to appropriately identify arterioles and venules, indicated by two different colors of the lines generated by the program, red for arterioles and blue for venules. The grader subsequently checks whether all the arterioles and venules are correctly identified and the software allows the grader to make any corrections if required (Fig. 3b).

## Technical Brief of the Parameters

1. Vessel caliber (summary) is represented by the central retinal arteriolar equivalent (CRAE) and the central retinal venular equivalent (CRVE), and caliber summaries of the largest six arterioles or venules.[17,18]
2. Vessel tortuosity, a reflection of the shape of the vessel, is expressed as a tortuosity index.[19] We used two measures of vessel tortuosity: simple and curvature. Simple tortuosity was a ratio between the actual length of a vessel segment and the shortest distance within the same segment. Curvature tortuosity was calculated from the integral of the total squared curvature along the path of the vessel, divided by the total arc length.[19]
3. Branching angle (in degrees) represented the angle between two daughter vessels.[20]
4. LDR is calculated as the length from the midpoint of the first branch to the midpoint of the second branch, divided by the diameter of the parent vessel at the first branch.[7]
5. Optimality deviation reflects the deviation of the vessel branching from the optimal configuration. Optimality of the vessel network at branching ($x$, junctional exponent)[20] is determined by the caliber sizes of two daughter vessels relative to the parent vessel and calculated as $d_1^x + d_2^x = d_0^x$, where $d_0$, $d_1$, and $d_2$ are diameters of the parent, larger, and smaller daughter vessels, respectively.[21] The greater the value of $x$, the larger the daughter arterioles are relative to the parent vessel. It has been proposed that in an optimal state, the value of the junctional exponent is 3,[20,22] and optimality deviation represents the deviation from this value.

## Statistical Analysis

Statistical analyses were performed using a commercial data analysis and statistical software package (Intercooled Stata 10.1 for Windows; Stata Corp., Lake Station, TX). The variance measuring the difference between each image and the reference image was used for the analysis because it eliminates the interindividual difference of retinal vascular geometric measures. Log-transformation was applied to LDR. All parameters were analyzed using repeated-measures ANOVA with post hoc multiple comparison tests to compare the mean value of each parameter from different frames over the cardiac cycle and to estimate the *P* value for variation of a particular parameter across different points in the cycle. Fractional polynomial regression was also performed to test for any nonlinear trends in each parameter during the cardiac cycle.[23]

# Results

Figure 4 shows the trend of the variation of the vessel diameter over the cardiac cycle. Both individual vessels and summary measures (CRAE and CRVE) showed similar patterns, where arterioles peaked before venules. Furthermore, CRAE became

narrowest when the CRVE peaked. Although variations for individual arteriolar and venular diameters were statistically significant ($P < 0.001$), both CRAE and CRVE did not show significant variation over the multiple images recorded over the cardiac cycle (all values of $P > 0.05$). Other retinal vascular geometry parameters have not been shown because there was no observable trend.

The Table shows the mean value and the absolute variation (in percentage values) of each parameter from images recoded at different points in the cardiac cycle. Overall, there was no significant variation found for arteriolar or venular parameters across different cardiac points (all values for variations, $P > 0.1$; for nonlinear trends, $P > 0.8$) except when the vessel diameter was measured individually ($P < 0.001$). The variation of the arteriolar and venular tortuosity between different images recorded at different points in the cardiac cycle was the smallest (variations range: 0–1.5%), compared with caliber (0–4.1%), branching angle (0–3.5%), LDR (0–2%), and optimality deviation (0–37%). Optimality deviation of both arterioles and venules showed the most variations compared with other parameters.

## Discussion

In this study, we have demonstrated that there was a significant variation in the diameter of individual retinal vessels over a cardiac cycle in generally healthy volunteers, and both the arterioles and venules were affected. The diameter variation followed a trend, where the diameter of the arterioles peaked close to the R-wave, whereas the peak of the venules diameter occurred midway between the systolic and diastolic. Our results also showed that vessel caliber summary (CRAE and CRVE) and other geometric parameters (vessel tortuosity, branching angle, LDR, and optimality deviation) of the retinal vasculature measured from fundus photographs using SIVA had none or little nonsignificant variation across different time points during the cardiac cycle, suggesting that these geometric parameters are unlikely to be influenced by physiologic changes during normal cardiac rhythm and other measurement differences.

The retinal vasculature is a unique site where there is a lack of autonomic nerve supply and scarce muscular components, unlike other vascular beds elsewhere in the body.[24] It has been suggested that the geometric organization of the retinal vasculature is controlled by a local autoregulation system, to adjust to a concurrent hemodynamic setting.[11] Any fluctuations in retinal blood flow may therefore geometrically alter the retinal vasculature to maintain local blood circulation in an optimal manner (maximum blood supply and diffusion with the least amount of energy).[25]

During the cardiac cycle, there are variations in blood velocity entering the eyeball. The blood velocity in the main supplying vessels of the retina, ophthalmic artery, and central retinal artery, at the peak-systolic are 3- to 4-fold higher than that at the end-diastolic phase.[11] This difference may explain some variations in vessel caliber as observed by us and demonstrated in earlier studies,[13,14] which showed a specific pattern following systolic and diastolic phases for individual vessels. However, these were not significant when we used the Parr–Hubbard formula, which summarized measures from the six largest arterioles and venules into an index of each vessel type; therefore, the index appears to be robust against the variability occurring in each individual vessel.[17,18] Sizable variation in optimality deviation is plausible since optimality deviation was determined by the caliber of two branches relative to the caliber of the parent vessel, from which combinations of errors are magnified by the power of 3.[9,20,22] On the other hand, recent evidence by Moret and associates[26] suggested that spontaneous pulsation in retinal vasculature does exist in some individuals, which could be another explanation to our findings, but requires further study.

During the cardiac cycle, both the individual vessels and their summary measures (CRAE or CRVE) showed a specific pattern of variations, although the summary measures were not statistically significant. However, in contrast, tortuosity, branching angle, and LDR did not demonstrate any pattern. The reason for the different pattern of variations in caliber than that in other parameters during the cardiac cycle is yet to be determined. According to Poiseuille's law, it has been hypothesized that changes in diameter size constitute the earliest form of vascular responses to blood flow changes.[27] We speculate that changes in vessel tortuosity, branching angle, and LDR may represent a further stage of vascular adaptation subsequent to changes in caliber size. Previous evidence proposed that increased vessel tortuosity is observed when the intravascular pressure increases beyond the elasticity limit of the vessel after vessel dilatation, as a compensatory mechanism to prevent exceeding capillary resistance,[28] which supports the current findings. Additionally, an animal experiment also showed that fluctuating blood flow may trigger branching remodeling, appear as an increased/decreased angle, to maintain a steady and optimal flow to target tissue.[29] Therefore, these parameters (tortuosity, branching, or LDR) might be less sensitive to subtle hemodynamic changes than caliber, but possibly more specific to adverse changes associated with some diseases (e.g., diabetes, cardiovascular diseases). This is an area needing further studies.

The strength of this study includes its automatic capture of sequences of nine images taken from the same eye using an ECG-synchronized retinal camera, and automatic retinal grading supervised by a single grader, whereas other images of the same eye were masked from the grader. Therefore, our results reflect high reproducibility of this measurement technique. The post hoc power analysis shows that our study should have over 80% study power to detect as little as 0.7% variations during the cardiac cycle in caliber or other vessel parameters. However, limitation is also noted. There may be subtle changes in single vessel or local region of the retinal vasculature of these parameters associated with the cardiac cycle that are masked by our summary measures. Therefore, further studies to compare these summary measures with individual vessel measures are needed.

In conclusion, our study showed although there was a small but significant change in the individual vessel caliber over the cardiac cycle, the vessel caliber summaries (CRAE, CRVE) and static retinal vascular geometric measures (tortuosity, branching angle, LDR, and optimality deviation) quantitatively measured from retinal images using SIVA, were relatively consistent across different cardiac points. Importantly, our study supports previous findings that there are small but significant changes to the caliber of individual vessels over the cardiac cycle, although these changes are not significant when the summary of the vascular caliber using the Parr–Hubbard formula, tortuosity, branching angle, and LDR are considered. These summary measurements are associated with several diseases and are likely due to pathophysiologic processes than normal physiologic variations during the cardiac cycle. Future studies exploring the clinical performance (e.g., sensitivity, specificity) of these parameters as subclinical markers for systemic vascular diseases (e.g., cardiovascular diseases, diabetes) are warranted.

## *References*

1. Wong TY, Hubbard LD, Klein R, et al. Retinal microvascular abnormalities and blood pressure in older people: the

Cardiovascular Health Study. *Br J Ophthalmol*. 2002;86:1007–1013.

2. Wong TY, Klein R, Sharrett AR, et al. Retinal arteriolar diameter and risk for hypertension. *Ann Intern Med*. 2004;140:248–255.
3. Cheung CY-l, Zheng Y, Hsu W, et al. Retinal vascular tortuosity, blood pressure, and cardiovascular risk factors. *Ophthalmology*. 2011;118:812–818.
4. Wong TY, Klein R, Sharrett AR, et al. Retinal arteriolar narrowing and risk of coronary heart disease in men and women. *JAMA*. 2002;287:1153–1159.
5. Witt N, Wong TY, Hughes AD, et al. Abnormalities of retinal microvascular structure and risk of mortality from ischemic heart disease and stroke. *Hypertension*. 2006;47:975–981.
6. Wong TY, Klein R, Sharrett AR, et al. Retinal arteriolar narrowing and risk of diabetes mellitus in middle-aged persons. *JAMA*. 2002;287:2528–2533.
7. Sasongko MB, Wang JJ, Donaghue KC, et al. Alterations in retinal microvascular geometry in young type 1 diabetes. *Diabetes Care*. 2010;33:1331–1336.
8. Sasongko M, Wong T, Nguyen T, Cheung C, Shaw J, Wang J. Retinal vascular tortuosity in persons with diabetes and diabetic retinopathy. *Diabetologia*. 2011;54:2409–2416.
9. Zamir M, Medeiros J, Cunningham T. Optimality principles in arterial branching. *J Theor Biol*. 1976;62:227–251.
10. Kawasaki R, Che Azemin MZ, Kumar DK, et al. Fractal dimension of the retinal vasculature and risk of stroke: a nested case-control study. *Neurology*. 2011;76:1766–1767.
11. Riva CE, Schmetterer L. Microcirculation of the ocular fundus. In: Tuma RF, Duran WN, Ley K, eds. *Handbook of Physiology: Microcirculation*. Amsterdam: Elsevier; 2008:735–765.
12. Dumskyj MJ, Aldington SJ, Dore CJ, et al. The accurate assessment of changes in retinal vessel diameter using multiple frame electrocardiograph synchronised fundus photography. *Curr Eye Res*. 1996;15:625–632.
13. Knudtson MD, Klein BEK, Klein R, et al. Variation associated with measurement of retinal vessel diameters at different points in the pulse cycle. *Br J Ophthalmol*. 2004;88:57–61.
14. Chen HC, Patel V, Wiek J, Rassam SM, Kohner EM. Vessel diameter changes during the cardiac cycle. *Eye*. 1994;8:97–103.
15. Gao XW, Bharath A, Stanton A, Hughes A, Chapman N, Thom S. Quantification and characterisation of arteries in retinal images. *Comput Methods Programs Biomed*. 2000;63:133–146.
16. Stewart CV, Chia-Ling T, Roysam B. The dual-bootstrap iterative closest point algorithm with application to retinal image registration. *IEEE Trans Med Imaging*. 2003;22:1379–1394.
17. Hubbard LD, Brothers RJ, King WN, et al. Methods for evaluation of retinal microvascular abnormalities associated with hypertension/sclerosis in the atherosclerosis risk in communities study. *Ophthalmology*. 1999;106:2269–2280.
18. Knudtson MD, Lee KE, Hubbard LD, Wong TY, Klein R, Klein BE. Revised formulas for summarizing retinal vessel diameters. *Curr Eye Res*. 2003;27:143–149.
19. Hart WE, Goldbaum M, Cote B, Kube P, Nelson MR. Measurement and classification of retinal vascular tortuosity. *Int J Med Inform*. 1999;53:239–252.
20. Zamir M, Medeiros JA, Cunningham TK. Arterial bifurcations in the human retina. *J Gen Physiol*. 1979;74:537–548.
21. Stanton AV, Wasan B, Cerutti A, et al. Vascular network changes in the retina with age and hypertension. *J Hypertens*. 1995;13:1724–1728.
22. Patton N, Maini R, MacGillivary T, Aslam TM, Deary IJ, Dhillon B. Effect of axial length on retinal vascular network geometry. *Am J Ophthalmol*. 2005;140:e641–e647.
23. Greenland S. Dose-response and trend analysis in epidemiology: alternatives to categorical analysis. *Epidemiology*. 1995;6:356–365.
24. Maenhaut N, Boussery K, Delaey C, Van De Voorde J. Control of retinal arterial tone by a paracrine retinal relaxing factor. *Microcirculation*. 2007;14:39–48.
25. Murray CD. The physiological principle of minimum work: I. The vascular system and the cost of blood volume. *Proc Natl Acad Sci U S A*. 1926;12:207–214.
26. Moret F, Poloschek CM, Lagreze WA, Bach M. Visualization of fundus vessel pulsation using principal component analysis. *Invest Ophthalmol Vis Sci*. 2011;52:5457–5464.
27. Pries AR, Secomb TW. Blood flow in microvascular networks. In: Tuma RF, Duran WN, Ley K, eds. *Handbook of Physiology: Microcirculation*. Amsterdam: Elsevier; 2008:735–765.
28. Kylstra J, Wierzbicki T, Wolbarsht M, Landers M, Stefansson E. The relationship between retinal vessel tortuosity, diameter, and transmural pressure. *Graefes Arch Clin Exp Ophthalmol*. 1986;224:477–480.
29. Djonov VG, Kurz H, Burri PH. Optimality in the developing vascular system: branching remodeling by means of intussusception as an efficient adaptation mechanism. *Dev Dyn*. 2002;224:391–402.